Precession of bounded orbits and shadow in quantum black hole spacetime

Yong-Zhuang Li[1,*] and Xiao-Mei Kuang[2,†]

[1]*Research center for theoretical physics, School of Science, Jiangsu University of Science and Technology, Zhenjiang 212003, China*

[2]*Center for Gravitation and Cosmology, College of Physical Science and Technology, Yangzhou University, Yangzhou 225009, China*

(Received 19 November 2022; accepted 2 March 2023; published 22 March 2023)

The geodesics around compact objects are one of the best tools to understand the geometrical properties of the central gravity source. In this paper, we study timelike and lightlike geodesics of a quantum black hole proposed in [E. Binetti *et al.*, Phys. Rev. D **106**, 046006 (2022).], which does not require committing to a specific model of quantum gravity. We analyze the quantum correction on the related obsrevables: periapsis precession of bounded orbits and angular shadow size. We find that, compared to the classical case, the quantum correction will enhance the periapsis precession as well as the black hole shadow. This effect is more significant for a smaller quantum black hole.

DOI: 10.1103/PhysRevD.107.064052

I. INTRODUCTION

As the most ambitious goal of physicists, the Grand Unified Theory intends to unite the gravitational and the other three interactions under the same framework, which inevitably requires a quantized theory of gravity. To date, Einstein's general relativity (GR) has been a very successful theory in modern physics and has passed plenty of test in astrophysics as well as astronomy. In particular, as a prediction of GR, black holes provide natural laboratories to test gravity in the strong field regime. Recent observations on gravitational waves [1–3] and the Event Horizon Telescope (EHT) on the shadow of supermassive M87* [4–6] and SgrA* [7,8] black holes further demonstrate the great success of GR. Nevertheless, GR is still facing challenges, such as the existence of the closed timelike curve [9], the nonlocality of gravitational field energy, etc. Especially, it breaks down inside the interior of event horizon and at the spacetime singularity. To address the problems at the singularities and event horizon, we should construct a self-consistent and complete theory of quantum theory. In this scenario, plenty of efforts have been made to invent black holes with quantum characteristics in various frameworks, such as noncommutative geometry [10,11], the loop quantum gravity [12,13], the effective field theories [14,15], and the renormalization group [16–18].

Since the strong gravity regime near a black hole is thought to be a region that may be helpful for exploring the quantum nature of the spacetime, it is unsurprising that the related theoretical studies on the optical obsevabational predictions, particularly the strong gravitational lensing effect and black hole shadow, of quantum effects on such black holes in various quantum gravity theories have been widely extended [19–36]. Those studies disclosed the print of the quantum effects on the strong gravitational effects of black hole, leading to an optimistic conclusion that quantum gravity effects could be accessible in the black holes' observations, especially from the shadow and photon ring of Sgr A* by EHT as proposed by Steven B. Giddings in 2014 [37].

The remarkable progress on the orbital evolution of S-stars orbiting the central object and the black hole image of Sgr A* shows the experimental ability to observe the vicinity of black holes. In the theoretical aspect, on one hand, the general relativistic effect promotes the elliptic orbit to rotate in the same direction as the orbital evolution, known as the periapsis precession of bound orbits [38]. Then, we could evaluate various contributions to the gravitational source field by observing the displacement of the orbit due to the precession and inversely diagnose the properties of the center gravity sources; see, for example, Refs. [39–44] and references therein. On the other hand, the shadow region due to the strong gravitational lensing effect, surrounded by a bright ring, is one of the important features in the black hole image. In detail, there is a photon region around the black hole, where the light rays from the light source are captured such that they cannot form an image visible to an outside observer. However, such a photon region could be dynamically unstable under perturbations, which allows light to encircle the black hole any number of times before being either scattered back to infinity or falling

*liyongzhuang@just.edu.cn
†Corresponding author.
xmeikuang@yzu.edu.cn

into the black hole [45]. If there exists only one unstable photon region, the photons which escape from the spherical orbits will form the appearance of the dark silhouette of the black hole, known as a black hole shadow from the external observers. Evidently, the shadow size is determined by photon region and position of the observer, so the angular size becomes a key measurement, which could characterize the properties of center black hole for the position-fixed observer. Thus, it is also widely discussed that the black hole shadow can provide the information on the central black holes; see Refs. [45–47] for reviews.

In this paper, we will focus on a quantum black hole in the effective theory which does not require committing to a specific model of quantum gravity, proposed very recently in Ref. [48]. In their approach, the quantum correction to the black hole physics was claimed to be captured, and the physical quantities can be well expanded in terms of the inverse powers of the black hole mass. Then, it is natural to investigate the prints of the general form of quantum correction on the observables of black hole, especially those related with the geodesics. Thus, the aim of this paper is to partly address the issues. We mainly investigate the quantum effects on the periapsis precession of a bound orbit of stars and shadow cast by analyzing the timelike or null-like geodesic in the quantum black hole spacetime.

As we mentioned before, there exist many works on geodesics and the related observables in the black hole spacetimes with quantum corrections. But those discussions highly depend on the models of quantum gravity, and an expected conclusion is still missing. The studies on the geodesics for the quantum black hole without requiring committing to a specific model of quantum gravity would shed light on the universal properties of quantum corrections on such geodesics. Moreover, these studies can provide theoretical prediction on the related observables, which we hope to be comparable with the possible future observations on the quantum effects in astrophysics and astronomy.

This paper is organized as follows. In Sec. II, we start by a briefly introduction to the quantum black hole investigated in Ref. [48]. In Secs. III and IV, we discuss the effects of the leading order quantum correction on the timelike and null-like geodesics. Conclusions and discussions are offered in Sec. V.

II. QUANTUM SCHWARZSCHILD BLACK HOLE

In this section, we will provide a brief review about the quantum black hole spacetime in an effective field theory investigated in Ref. [48], which is considered as the deviation from classical case. For a Schwarzschild black hole metric

$$ds^2 = -f(r)dt^2 + \frac{dr^2}{f(r)} + r^2(d\theta^2 + \sin^2\theta d\psi^2),$$

$$\text{with} \quad f(r) = 1 - \frac{2G_N M}{r}, \tag{1}$$

if one takes the dimensionless quantities

$$z \coloneqq M_P r = \frac{r}{\ell_P}, \qquad \chi \coloneqq \frac{M}{M_P}, \tag{2}$$

with ℓ_P the Planck length, M_P the Planck mass, and $G_N M_P^2 = 1$, one then obtains the redshift function as

$$f(r) = f_0(z) = 1 - 2\chi/z. \tag{3}$$

Following the physical procedures in Ref. [48], one can upgrade the classical metric (1) into a quantum one as

$$ds^2 = -f(z)dt^2 + \frac{dz^2}{f(z)} + z^2(d\theta^2 + \sin^2\theta d\varphi^2), \tag{4}$$

with

$$f(z) = 1 - \frac{2\chi}{z}\sum_{n=0}^{\infty}\frac{\Omega_n}{d(z)^{2n}}, \tag{5}$$

where the dimensionless coefficients Ω_n are specified by a given theory of quantum gravity with $\Omega_0 = 1$ and

$$d(z) \coloneqq \int_0^z dz'/\sqrt{|f(z')|} \tag{6}$$

is the normalized proper distance from the center of the black hole. Therefore, for the zero-order case, one could reproduce the classical proper distance

$$\begin{aligned} d_0(z) &= \int_0^z \frac{dz'}{\sqrt{|1-\frac{2\chi}{z'}|}} \\ &= \begin{cases} \pi\chi - 2\chi\tan^{-1}\sqrt{\frac{2\chi}{z}-1} - \sqrt{z(2\chi - z)} & , \quad 0 < z < 2\chi \\ \pi\chi & , \quad z = 2\chi \\ \pi\chi + 2\chi\tanh^{-1}\sqrt{1-\frac{2\chi}{z}} + \sqrt{z(z-2\chi)} & , \quad 2\chi < z < \infty. \end{cases} \end{aligned} \tag{7}$$

Subsequently, by combining (5)–(7), one can derive the quantum proper distance of any order, as well as the redshift function of the black hole with quantum corrections of various orders. Readers can refer to Ref. [48] for more details. Here, we are interested in the quantum black hole with leading-order quantum correction, so (5) reads as

$$f(z) = 1 - \frac{2\chi}{z}\left[1 + \frac{\Omega_1}{d_1^2(z)}\right], \tag{8}$$

where $d_1(z)$ is the leading-order quantum proper distance

$$d_1(z) = \int_0^z \frac{dz'}{\sqrt{\left|1 - \frac{2\chi}{z'}\left[1 + \frac{\Omega_1}{d_0^2(z')}\right]\right|}}. \tag{9}$$

It is obvious that as $\Omega_1 \to 0$, redshift function (8) reduces to the classical Schwarzschild case (3).

Next, we shall study the periapsis precession of bounded orbits and angular shadow size affected by the leading-order quantum correction. In general, the sign of Ω_1 could be arbitrary. However, negative Ω_1 corresponds to two horizons (inner and outer ones), while for positive Ω_1, $f(z) = 0$ has single solution. Therefore, in order to compare closely with the classical Schwarzschild case, we will consider only the case with $\Omega_1 > 0$, which leads to a single horizon. Samples of $d_1(z)$ for various χ and Ω_1 are numerically shown in Fig. 1. Especially, we plot the quantum correction term $\Omega_1/d_1^2(z)$ as a function of χ with the fixed ratio $z/\chi = 3$ which corresponds to the radius of photon sphere $r_{\rm ps}$ in a classical Schwarzschild black hole (where $r_{\rm ps} = 3M$).

III. TIMELIKE GEODESIC

Following conventional method, for the metric (4) and (8), we have two constants of motion

$$E = f(z)\dot{t}, \qquad L = z^2 \sin\theta^2 \dot{\varphi}, \tag{10}$$

indicating the energy and angular momentum of the particle, respectively. The dot is respect with the affine parameter. For a timelike geodesic, the constraint on the trajectories is given by $g_{\mu\nu}v^\mu v^\nu = -1$, i.e.,

$$-1 = -f(z)\dot{t}^2 + \frac{\dot{z}^2}{f(z)} + z^2(\dot{\theta}^2 + \sin^2\theta\dot{\varphi}^2). \tag{11}$$

Due to the spherical symmetry of the metric, we are safe to consider the equatorial plane, i.e., $\theta = \pi/2$. Substituting Eq. (10) into Eq. (11), we can obtain that the trajectory of the particle is uniquely determined by

$$\left(\frac{dz}{d\varphi}\right)^2 = \frac{z^4}{L^2}(E^2 - V_{\rm eff}^2), \tag{12}$$

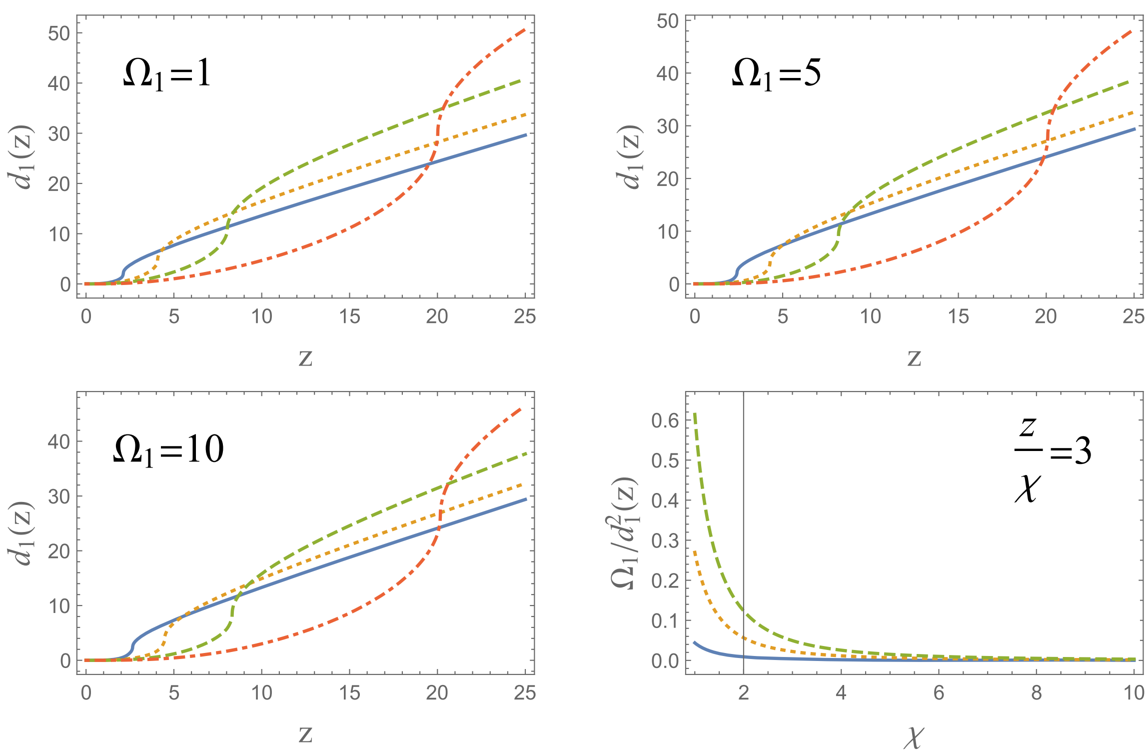

FIG. 1. The behavior of $d_1(z)$ with different Ω_1 and χ. For the first three panels, we choose $\chi = 1$ (the solid blue line), $\chi = 2$ (the dotted orange line), $\chi = 4$ (the dashed green line), and $\chi = 10$ (the dot-dashed red line). For the right-bottom panel, we plot the quantum correction term $\Omega_1/d_1^2(z)$ as a function of χ with the fixed ratio $z/\chi = 3$ for $\Omega_1 = 10, 5, 1$ (top to bottom).

with the definition of effective potential

$$V_{\mathrm{eff}}^2 = f(z)\left(1+\frac{L^2}{z^2}\right). \tag{13}$$

With different values of L, we plot the effective potential for selected parameters Ω_1 and χ; please see Fig. 2. It shows that the quantum effect has a more significant impact on small mass black holes. See also Fig. 3, where we show the difference of the effective potential between quantum and classical Schwarzschild black holes.

For some simplification, we can rewrite Eq. (12) in terms of $u = z^{-1}$, which leads to

$$\left(\frac{du}{d\varphi}\right)^2 = 2u^3\chi(1+M(u)) - u^2 + \frac{2u\chi}{L^2}(1+M(u)) - \frac{1-E^2}{L^2}, \tag{14}$$

where the quantum-corrected function

$$M(u) \coloneqq \frac{\Omega_1}{d_1^2(u^{-1})}. \tag{15}$$

For $\Omega_1 = 0$, the above equation will reproduce the classical timelike geodesic equation (see the detailed discussion in Chapter 3 of Ref. [49]). However, for the quantum black hole with $\Omega_1 \neq 0$, unlike the classical one, the analytical solution to Eq. (14) can be hardly found, even following the approach shown in Refs. [50,51]. We have to benefit from the numerical method to investigate the effect of quantum term on the trajectories of the particle.

A. Bound orbits

For Eq. (14), the particle trajectories are controlled by three parameters L, E, Ω_1 for fixed χ. In addition, the effective potential is relevant to parameters L and Ω_1 for fixed χ. Thus, the bounded trajectories will be determined by disposition of the roots of the equation $V_{\mathrm{eff}}^2(z) = E^2$. There is an extensive literature that has discussed the classification of the geodesic in different spacetimes [41,49–59]. In this work, we will focus on the case $1 > E^2 > V_{\mathrm{eff}}^2(z; L_s)$, which will ensure the existence of the bound orbits [49]. L_s is exclusively confirmed for fixed Ω_1 and χ such that

$$\frac{dV_{\mathrm{eff}}^2}{dz} \ \text{is a monotonic function and} \ \left.\frac{dV_{\mathrm{eff}}^2}{dz}\right|_{z=z_s} = 0. \tag{16}$$

z_s is the critical point.

In Figs. 4 and 5, we numerically figure out the bound trajectories for various parameters (L, E, Ω_1, χ). Evidently, we can draw the following conclusions:

(i) For small black hole, the quantum term will have a relatively greater influence on the bounded orbits. In other words, with larger quantum corrections come greater deviation from the standard bounded orbits.

(ii) For large black hole, the deviation is only obvious when the quantum corrections are relatively large.

Those properties are reasonable as they are consistent with the corresponding effects on the quantum corrections terms we found in Fig. 1.

B. Periapsis precession

We now consider another physical concept, the periapsis precession, which is defined as

$$\Delta_{\mathrm{per}} = 2\int_{z_{\mathrm{per}}}^{z_{\mathrm{ap}}} \frac{d\varphi}{dz} dz - 2\pi, \tag{17}$$

where z_{ap}, z_{per} are the real solutions of $E^2 = V_{\mathrm{eff}}^2(r)$, standing for the radii of an apoapsis and a periapsis, respectively [41,60]. This concept states that the periapsis shifts forward (or backward) by an angle Δ_{per} with each circuit around the ellipse. In Table I, we list the periapsis precession for selected parameter sets. Again, such results demonstrate the previous conclusion that only large enough quantum terms have relatively significant influences on the bounded orbits.

IV. NULL GEODESIC

We move on to study the motion of photons, the rays of which could be strongly deflected and even travel on the circular orbits as they pass close to the black hole. Therefore, the black hole is seen as a dark disk in the sky, known as a black hole shadow. It is the photon region (consisting of rays with unstable circular obits) but not the horizon that determines the shadow. For spherically symmetric and static spacetime, the photon region reduces to the photon sphere, and the shadow is a perfect circle; therefore, their unique character is the size or radius. Thus, we shall explore the quantum effect on the sizes of the photon sphere and shadow for the quantum black hole spacetime (8).

A. Photon sphere

The photon sphere describes the unstable circular orbits outside the horizon, which confines the black hole image for observers at a distance. The trajectories of photon are described by the null geodesic, i.e., $g_{\mu\nu}v^\mu v^\nu = 0$, staying on a sphere. Following Ref. [46], such a sphere requires that

$$\frac{dz}{d\varphi} = 0, \qquad \frac{d^2z}{d\varphi^2} = 0. \tag{18}$$

Differentiating the null geodesic equation with respect to φ and combining the above conditions (18), we obtain

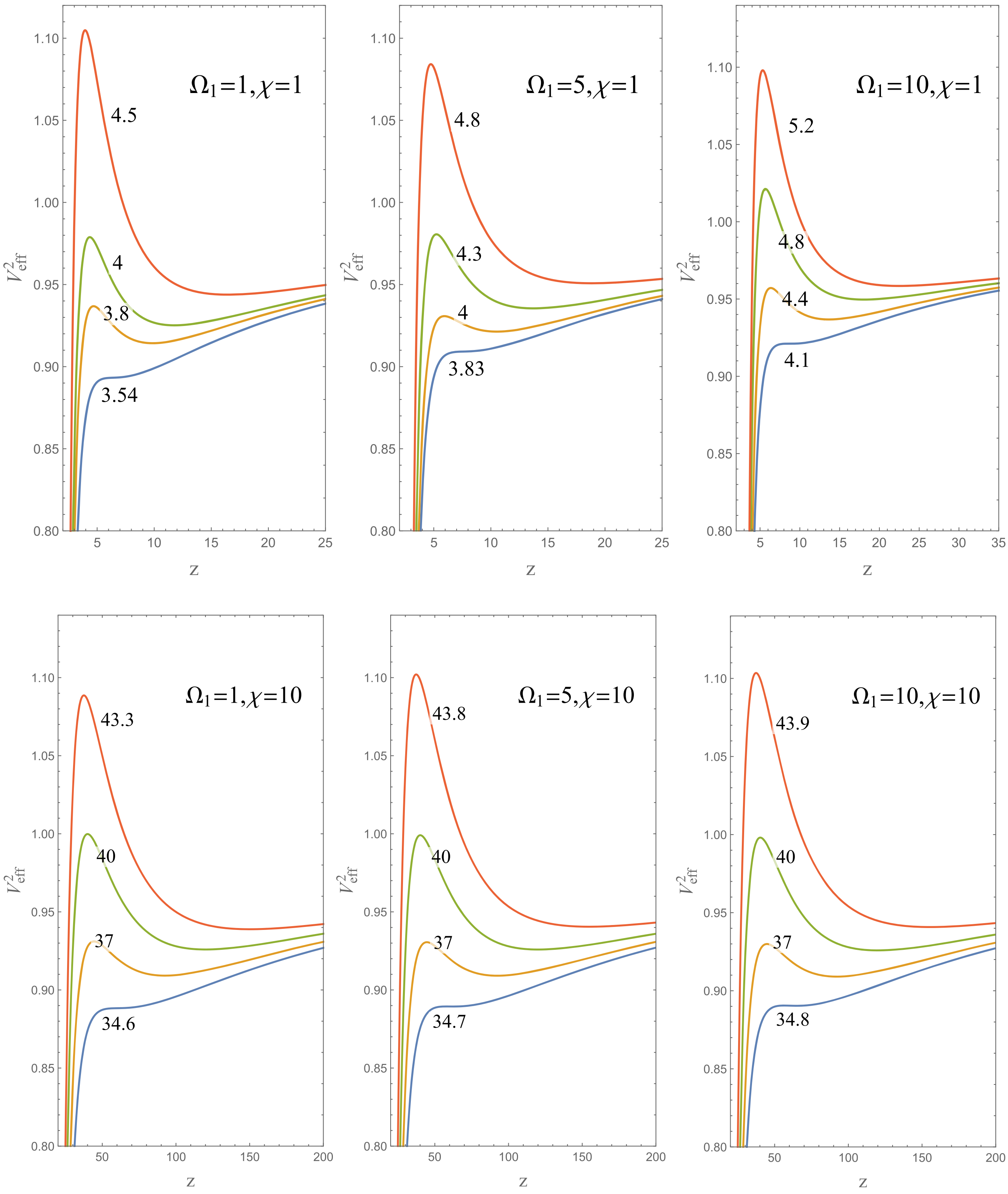

FIG. 2. The effective potential as a function of z for different L.

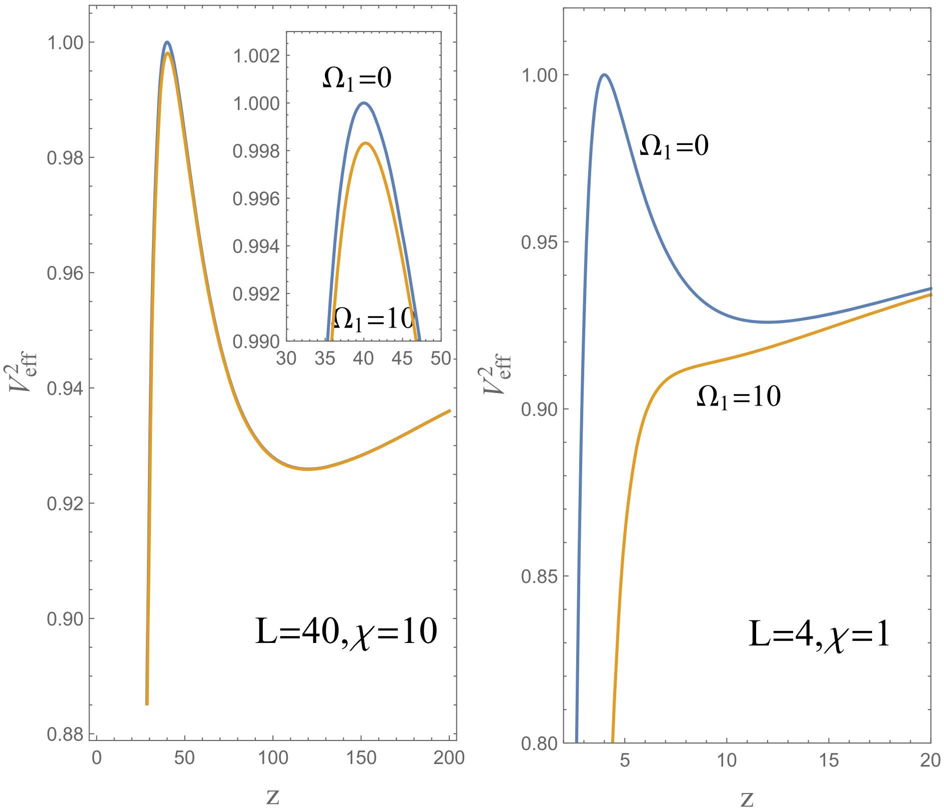

FIG. 3. The effective potential as a function of z for the quantum ($\Omega_1 = 10$) and classical ($\Omega_1 = 0$) Schwarzschild black hole.

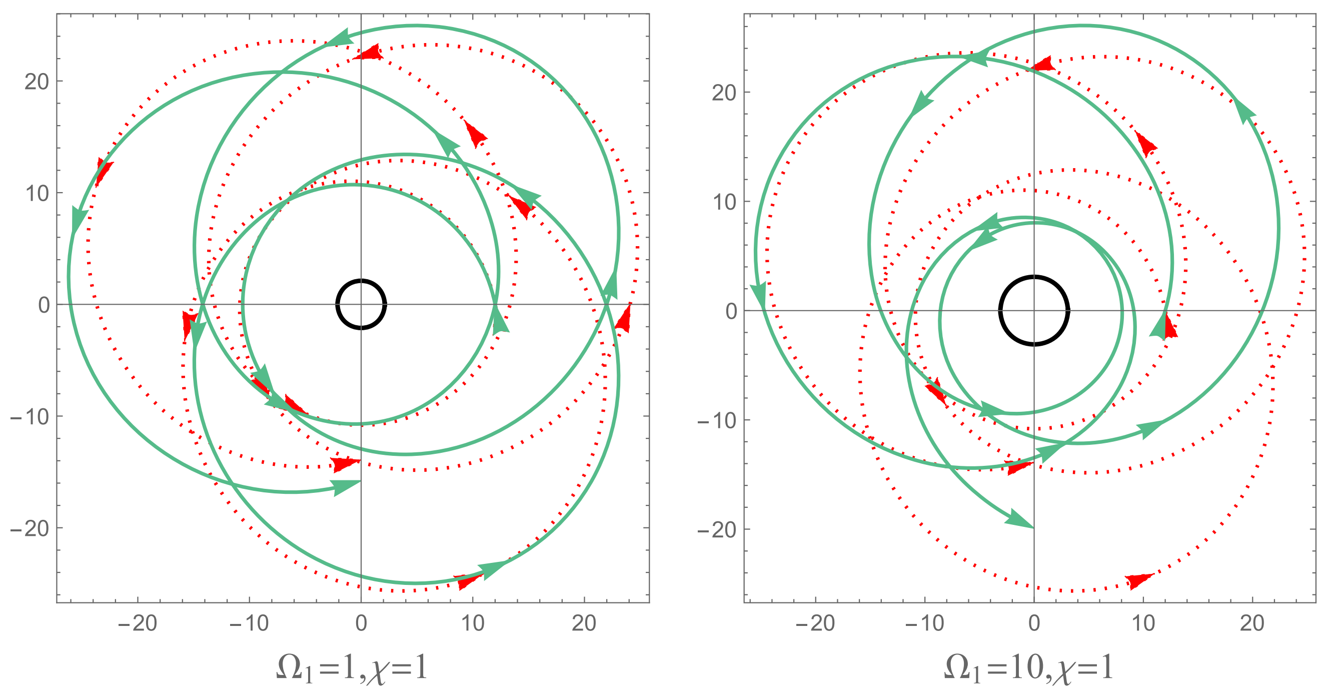

FIG. 4. The bounded orbits with periapsis precession. The green solid line indicates the bounded orbit with quantum correction, where the dotted red line stands for the bounded orbit for the standard Schwarzschild black hole. The other parameters are $E^2 = 0.95$, $L = 4.4$. The black circle means the horizon z_h with quantum corrections, (left) $z_h = 2.118$ and (right) $z_h = 2.651$.

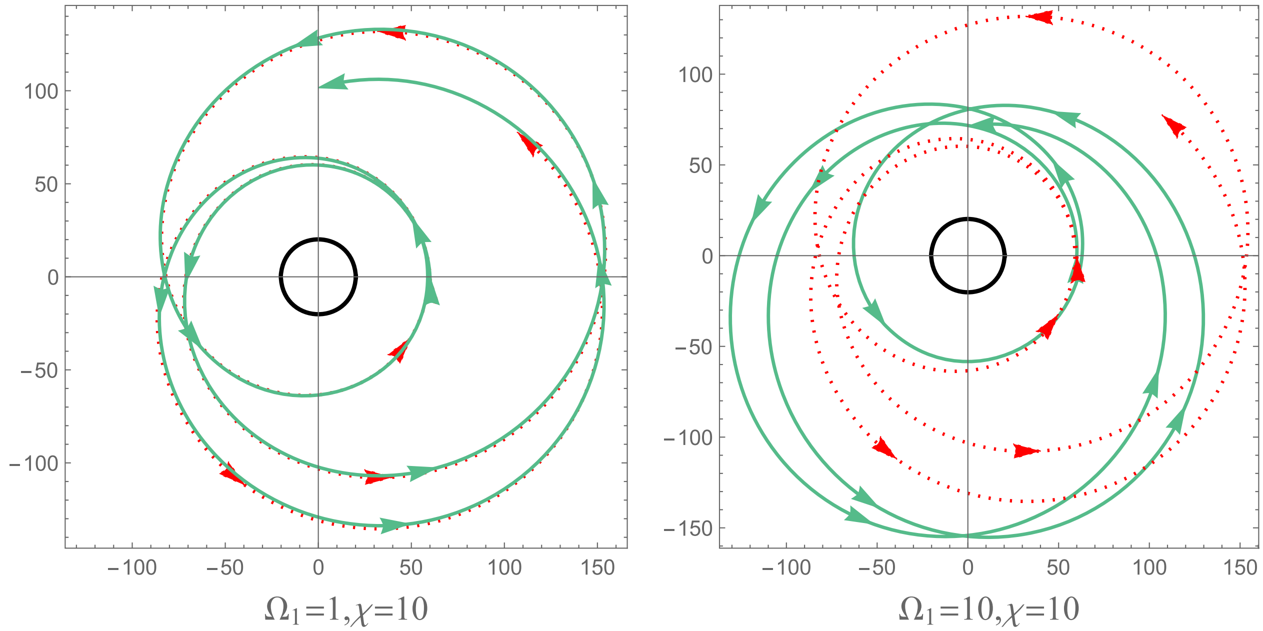

FIG. 5. The green solid line indicates the bounded orbit with quantum correction, where the dotted red line stands for the bound orbit for standard Schwarzschild black hole. The other parameters are $E^2 = 0.921$, $L = 37$. Left: $z_h = 20.019$; right: $z_h = 20.163$.

$$\frac{d}{dz} h^2(z) = 0, \tag{19}$$

where $h^2(z) = z^2/f(z)$. For a classical nonrotating spherically symmetric Schwarzschild black hole, the radius of photon sphere is given by $z_{\rm ps}^c = 3\chi$ [46].

In Fig. 6, we numerically plot the relative radius $\Delta z_{\rm ps} = z_{\rm ps} - 3\chi$ of the photon sphere as a function of Ω_1 for selected parameter χ, where $z_{\rm ps}$ is the radius of photon sphere with quantum corrections. It is obvious that the quantum correction Ω_1 will enlarge the photon sphere, and this phenomenon is more significant for a smaller quantum black hole.

B. Black hole shadow

To describe the shadow on a static observer's sky, it is more proper to employ the angular radius α_{sh} of the shadow rather than the shadow radius. For a Schwarzschild black hole, the angular radius is given by [61,62]

$$\sin^2\alpha_{\rm sh} = 27m^2\left(\frac{r_O - 2m}{r_O^3}\right), \tag{20}$$

where r_O is the observer's r coordinate from the black hole and $m = G_N M/c^2$ is the mass of black hole. For the case $r_O \gg m$, one has

$$\sin^2\alpha_{\rm sh} = \frac{27m^2}{r_O^2} + \mathcal{O}\left(\frac{m^3}{r_O^3}\right). \tag{21}$$

For the Schwarzschild metric with quantum corrections, the angular radius $\tilde{\alpha}_{\rm sh}$ can be written as

$$\sin^2\tilde{\alpha}_{\rm sh} = \frac{h^2(z_{\rm ps})}{h^2(z_O)}, \tag{22}$$

TABLE I. The periapsis precession $\Delta_{\rm per}$ for different parameters (χ, Ω_1, L, E^2).

χ	Ω_1	L	E^2	$\Delta_{\rm per}$
1	0	4.4	0.95	1.779
1	1	4.4	0.95	1.898
1	10	4.4	0.95	4.819
10	0	37	0.921	5.479
10	1	37	0.921	5.496
10	10	37	0.921	5.658

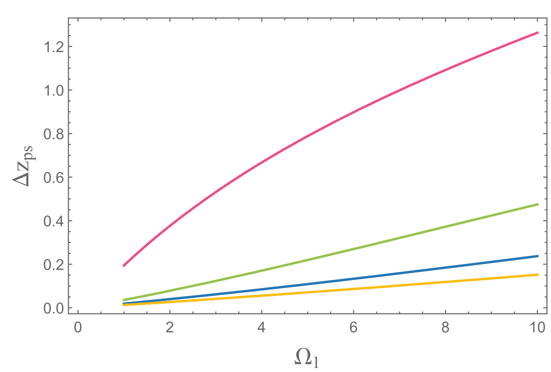

FIG. 6. The difference of radius of photon sphere $\Delta z_{\rm ps} = z_{\rm ps} - 3\chi$ as a function of Ω_1. From top to down, we set $\chi = 1, 4, 7, 10$.

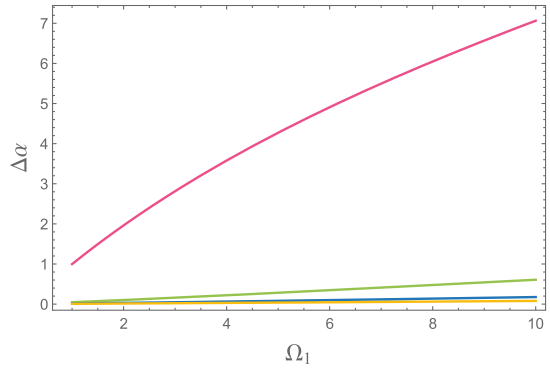

FIG. 7. The difference $\Delta\alpha = \tilde{\alpha}_{sh} - \alpha_{sh}$ of the angular radius with unit micro-arc-seconds as a function of Ω_1. For both panels from top to bottom, $\chi = 1, 4, 7, 10$.

where we have

$$h^2(z_O) = \frac{z_O^2}{1 - \frac{2\chi}{z_O}\left(1 + \frac{\Omega_1}{d_1^2(z_O)}\right)} \approx z_O^2 + \mathcal{O}\left(\frac{\chi}{z_O}\right). \tag{23}$$

The second approximation is due to the monotonicity of $d_1(z)$ from Fig. 1. Meanwhile, χ/z can be considered to have same physical connotation with m/r such that Eq. (22) is represented as

$$\sin^2\tilde{\alpha}_{sh} \approx \frac{\chi^2}{z_O^2}\frac{h^2(z_{ps})}{\chi^2}. \tag{24}$$

The observation of our Galaxy's supermassive black hole Sgr A* provides a best estimated mass $M \approx 4.1 \times 10^6 M_\odot$ and a distance $\sim$8.3 kpc for an observer on the Earth [63–67].[1] As an illustrative example, we can treat Sgr A* as a classical Schwarzschild black hole so the angular radius $\alpha_{sh} \approx 25$ micro-arc-seconds. In Fig. 7, we plot the difference of angular radius $\Delta\alpha = \tilde{\alpha}_{sh} - \alpha_{sh}$ as a function of Ω_1 using the above data. This result confirms once again that the quantum correction of spacetime is significant only in the case of small black holes, as indicated from the photon sphere.

V. CONCLUSIONS AND DISCUSSIONS

In this work, by analyzing the timelike and null geodesics in the quantum black hole spacetime, we numerically investigate the quantum effects on the observables like the periapsis precession of a bound orbit of stars and shadow cast. Such quantum corrections to the black hole physics are organized by the inverse powers of a physical distance and the dimensionless coefficients Ω_n, which are specified by a given quantum gravity. With the consideration of the leading-order quantum correction, the results confirm that the quantum effects are only evident for the relatively large ratio of Ω_1/χ. However, in the calculations, only small χ has been adopted. For massive black hole where χ has an extremely large order of magnitude, the coefficient Ω_1 has to be at least the same order as χ to generate the observable effects. For example, $\chi \sim 10^{44}$ for supermassive SgrA*, and our numerical calculation for such a case is extremely difficult. As was studied in various modified gravity theories [68–74], we are interested in further optimizing our numerical methods to study the constraint on Ω_1 from EHT observations on SgrA* but will leave it for future work. Anyhow, a non-negligible and notable point is to determine the physical properties of the quantum coefficients Ω_n with extremely large magnitude.

With the results obtained by investigating the characteristics of a quantum black hole, a crucial purpose is to distinguish the quantum black holes from classical ones through observation. Our results show that such deviations are detectable with improved resolution of the EHT once the black hole mass is preliminarily measured through various methods; see Refs. [75,76] for the supermassive and intermediate-mass black hole measurement. More specifically, the EHT observational data of the black hole shadow and the photon ring are not sufficient to determine the quantum parameters because the same result can be caused by quantum effects or by the classical black holes of different masses. For example, our calculations show that the radius of the photon ring increases with the quantum correction, while the larger the mass of a classical black hole, the larger the photon ring. However, once we can measure the black hole mass by other means, then we will be able to determine the parameter χ, from which we can further constrain the range of values of Ω_1.

Note that here we have focused on the single horizon quantum black hole with the first leading-order correction. In Ref. [48], more cases, such as a quantum black hole with two horizons in the first-order correction and black holes with higher-order quantum corrections, are addressed. They all exhibit more colorful geometrical properties with quantum corrections, so it would be interesting to extend our studies to these cases. In addition, the observed shadow images from the EHT collaborator of black holes M87* and Sgr A* are both compatible with the Kerr black hole. It will be natural to extend such an effective field approach to the Kerr black hole and study the properties of its null and timelike geodesics.

ACKNOWLEDGMENTS

This work is partly supported by Fok Ying Tung Education Foundation under Grant No. 171006 and Natural Science Foundation of Jiangsu Province under Grant No. BK20211601. Y.-Z. Li was also supported by the Jiangsu University of Science and Technology for Doctoral Research (Grant No. 1052931902).

[1]By adopting these data we have the ratio $\frac{m}{r_O} \sim 10^{-11}$.

[1] B. P. Abbott *et al.* (LIGO Scientific and Virgo Collaborations), Phys. Rev. Lett. **116**, 061102 (2016).
[2] B. P. Abbott *et al.* (LIGO Scientific and Virgo Collaborations), Phys. Rev. X **9**, 031040 (2019).
[3] B. P. Abbott *et al.* (LIGO Scientific and Virgo Collaborations), Astrophys. J. Lett. **892**, L3 (2020).
[4] K. Akiyama *et al.* (Event Horizon Telescope Collaboration), Astrophys. J. Lett. **875**, L1 (2019).
[5] K. Akiyama *et al.* (Event Horizon Telescope Collaboration), Astrophys. J. Lett. **875**, L4 (2019).
[6] K. Akiyama *et al.* (Event Horizon Telescope Collaboration), Astrophys. J. Lett. **875**, L5 (2019).
[7] K. Akiyama *et al.* (Event Horizon Telescope Collaboration), Astrophys. J. Lett. **930**, L12 (2022).
[8] K. Akiyama *et al.* (Event Horizon Telescope Collaboration), Astrophys. J. Lett. **930**, L17 (2022).
[9] S. W. Hawking, Phys. Rev. D **46**, 603 (1992).
[10] S. Ansoldi, P. Nicolini, A. Smailagic, and E. Spallucci, Phys. Lett. B **645**, 261 (2007).
[11] E. Spallucci, A. Smailagic, and P. Nicolini, Phys. Lett. B **670**, 449 (2009).
[12] R. Gambini and J. Pullin, Phys. Rev. Lett. **110**, 211301 (2013).
[13] R. Gambini and J. Pullin, Phys. Rev. Lett. **101**, 161301 (2008).
[14] N. E. J. Bjerrum-Bohr, J. F. Donoghue, and B. R. Holstein, Phys. Rev. D **68**, 084005 (2003); **71**, 069904(E) (2005).
[15] G. G. Kirilin, Phys. Rev. D **75**, 108501 (2007).
[16] A. Bonanno and M. Reuter, Phys. Rev. D **60**, 084011 (1999).
[17] M. Reuter and E. Tuiran, Phys. Rev. D **83**, 044041 (2011).
[18] A. Bonanno and M. Reuter, Phys. Rev. D **73**, 083005 (2006).
[19] S.-W. Wei, P. Cheng, Y. Zhong, and X.-N. Zhou, J. Cosmol. Astropart. Phys. 08 (2015) 004.
[20] A. Held, R. Gold, and A. Eichhorn, J. Cosmol. Astropart. Phys. 06 (2019) 029.
[21] R. Kumar, B. P. Singh, and S. G. Ghosh, Ann. Phys. (Amsterdam) **420**, 168252 (2020).
[22] C. Liu, T. Zhu, Q. Wu, K. Jusufi, M. Jamil, M. Azreg-Aïnou, and A. Wang, Phys. Rev. D **101**, 084001 (2020); **103**, 089902(E) (2021).
[23] T. Zhu and A. Wang, Phys. Rev. D **102**, 124042 (2020).
[24] S. Brahma, C.-Y. Chen, and D.-h. Yeom, Phys. Rev. Lett. **126**, 181301 (2021).
[25] Q.-M. Fu and X. Zhang, Phys. Rev. D **105**, 064020 (2022).
[26] X.-X. Zeng, G.-P. Li, and K.-J. He, Nucl. Phys. **B974**, 115639 (2022).
[27] R. Kumar Walia, arXiv:2207.02106.
[28] K. Jusufi, M. Azreg-Aïnou, M. Jamil, and Q. Wu, Universe **8**, 210 (2022).
[29] B. Gao and X.-M. Deng, Eur. Phys. J. C **81**, 983 (2021).
[30] X. Lu and Y. Xie, Eur. Phys. J. C **81**, 627 (2021).
[31] Z. Xu and M. Tang, Chin. Phys. C **46**, 085101 (2022).
[32] M. Afrin, S. Vagnozzi, and S. G. Ghosh, Astrophys. J. **944**, 149 (2023).
[33] R. A. Konoplya, Phys. Lett. B **804**, 135363 (2020).
[34] F. Atamurotov, M. Jamil, and K. Jusufi, Chin. Phys. C **47**, 035106 (2023).
[35] C. Zhang, Y.-G. Ma, and J.-S. Yang, arXiv:2302.02800v2.
[36] S. U. Islam, J. Kumar, R. K. Walia, and S. G. Ghosh, Astrophys. J. **943**, 22 (2023).
[37] S. B. Giddings, Phys. Rev. D **90**, 124033 (2014).
[38] S. Weinberg, *Gravitation and Cosmology* (Wiley, New York, 1972).
[39] G. V. Kraniotis, Classical Quantum Gravity **24**, 1775 (2007).
[40] S. Akcay, Phys. Rev. D **96**, 044024 (2017).
[41] K. Ota, S. Kobayashi, and K. Nakashi, Phys. Rev. D **105**, 024037 (2022).
[42] Mohammad Bagher Jahani Poshteh, Phys. Rev. D **106**, 044037 (2022).
[43] T. Igata, T. Harada, H. Saida, and Y. Takamori, arXiv: 2202.00202.
[44] M. Fathi, M. Olivares, and J. R. Villanueva, Eur. Phys. J. C **82**, 629 (2022).
[45] P. V. P. Cunha and C. A. R. Herdeiro, Gen. Relativ. Gravit. **50**, 42 (2018).
[46] V. Perlick and O. Yu. Tsupko, Phys. Rep. **947**, 1 (2022).
[47] M. Wang, S. Chen, and J. Jing, Commun. Theor. Phys. **74**, 097401 (2022).
[48] E. Binetti, M. Del Piano, S. Hohenegger, F. Pezzella, and F. Sannino, Phys. Rev. D **106**, 046006 (2022).
[49] S. Chandrasekhar, *The Mathematical Theory of Black Holes* (Oxford University Press, Oxford, 1982).
[50] E. Hackmann and C. Lämmerzahl, Phys. Rev. Lett. **100**, 171101 (2008).
[51] E. Hackmann, C. Lämmerzahl, V. Kagramanova, and J. Kunz, Phys. Rev. D **81**, 044020 (2010).
[52] J. Chen and Y. Wang, Int. J. Mod. Phys. A **25**, 1439 (2010).
[53] A. N. Chowdhury, M. Patil, D. Malafarina, and P. S. Joshi, Phys. Rev. D **85**, 104031 (2012).
[54] R. Zhang, S. Zhou, J. Chen, and Y. Wang, Gen. Relativ. Gravit. **47**, 128 (2015).
[55] A. B. Joshi, P. Bambhaniya, D. Dey, and P. S. Joshi, arXiv:1909.08873.
[56] P. Bambhaniya, A. B. Joshi, D. Dey, and P. S. Joshi, Phys. Rev. D **100**, 124020 (2019).
[57] P. Bambhaniya, J. S. Verma, D. Dey, P. S. Joshi, and A. B. Joshi, arXiv:2109.11137.
[58] D. N. Solanki, P. Bambhaniya, D. Dey, P. S. Joshi, and K. N. Pathak, Eur. Phys. J. C **82**, 77 (2022).
[59] A. M. Al Zahrani, Astrophys. J. **937**, 50 (2022).
[60] C. W. Misner, K. S. Thorne, and J. A. Wheeler, *Gravitation* (Freeman, San Francisco, 1973).
[61] J. L. Synge, Mon. Not. R. Astron. Soc. **131**, 463 (1966).
[62] Y. B. Zeldovich and I. D. Novikov, Sov. Phys. Usp. **8**, 522 (1966).
[63] A. M. Ghez, S. Salim, N. N. Weinberg, J. R. Lu, T. Do, J. K. Dunn, K. Matthews, M. R. Morris, S. Yelda, E. E. Becklin *et al.*, Astrophys. J. **689**, 1044 (2008).
[64] S. Gillessen, F. Eisenhauer, S. Trippe, T. Alexander, R. Genzel, F. Martins, and T. Ott, Astrophys. J. **692**, 1075 (2009).
[65] R. Abuter, A. Amorim, M. Bauböck, J. P. Berger, H. Bonnet, W. Brandner, Y. Clénet, V. Coudé du Foresto, P. T. de Zeeuw *et al.* (The GRAVITY Collaboration), Astron. Astrophys. **625**, L10 (2019).
[66] K. Akiyama, A. Alberdi *et al.* (Event Horizon Telescope Collaboration), Astrophys. J. Lett. **930**, L15 (2022).

[67] T. Do, A. Hees, A. M. Ghez, G. D. Martinez, D. S. Chu, S. Jia, S. Sakai, J. R. Lu, A. K. Gautam, K. K. O'Neil *et al.*, Science **365**, 664 (2019).
[68] Y. Meng, X.-M. Kuang, and Z.-Y. Tang, Phys. Rev. D **106**, 064006 (2022).
[69] S. Vagnozzi *et al.*, arXiv:2205.07787.
[70] C.-Y. Chen, Phys. Rev. D **106**, 044009 (2022).
[71] X.-M. Kuang, Z.-Y. Tang, B. Wang, and A. Wang, Phys. Rev. D **106**, 064012 (2022).
[72] Z.-Y. Tang, X.-M. Kuang, B. Wang, and W.-L. Qian, Sci. Bull. **67**, 2272 (2022).
[73] R. C. Pantig and A. Övgün, Ann. Phys. (Amsterdam) **448**, 169197 (2023).
[74] Y. Chen, R. Roy, S. Vagnozzi, and L. Visinelli, Phys. Rev. D **106**, 043021 (2022).
[75] B. M. Peterson, Space Sci. Rev. **183**, 253 (2014).
[76] J. E. Greene, J. Strader, and L. C. Ho, Annu. Rev. Astron. Astrophys. **58**, 257 (2020).